HAL
open science

Simplified approach to the repulsive Bose gas from low to high densities and its numerical accuracy

Eric A. Carlen, Markus Holzmann, Ian Jauslin, Elliott H. Lieb

To cite this version:

Eric A. Carlen, Markus Holzmann, Ian Jauslin, Elliott H. Lieb. Simplified approach to the repulsive Bose gas from low to high densities and its numerical accuracy. Physical Review A : Atomic, molecular, and optical physics [1990-2015], 2021, 103 (5), pp.053309. 10.1103/PhysRevA.103.053309 . hal-03368550

HAL Id: hal-03368550

https://cnrs.hal.science/hal-03368550

Submitted on 6 Oct 2021

HAL is a multi-disciplinary open access archive for the deposit and dissemination of scientific research documents, whether they are published or not. The documents may come from teaching and research institutions in France or abroad, or from public or private research centers.

L'archive ouverte pluridisciplinaire **HAL**, est destinée au dépôt et à la diffusion de documents scientifiques de niveau recherche, publiés ou non, émanant des établissements d'enseignement et de recherche français ou étrangers, des laboratoires publics ou privés.

Simplified approach to the repulsive Bose gas from low to high densities and its numerical accuracy

Eric A. Carlen,[1,*] Markus Holzmann,[2,3,†] Ian Jauslin,[4,‡] and Elliott H. Lieb[5,§]
[1]*Department of Mathematics, Rutgers University, Piscataway, New Jersey 08854, USA*
[2]*Univ. Grenoble Alpes, CNRS, LPMMC, 38000 Grenoble, France*
[3]*Institut Laue Langevin, BP 156, F-38042 Grenoble Cedex 9, France*
[4]*Department of Physics, Princeton University, New Jersey 08544, USA*
[5]*Departments of Mathematics and Physics, Princeton University, New Jersey 08544, USA*

(Received 29 November 2020; accepted 3 March 2021; published 7 May 2021)

In 1963, a simplified approach was developed to study the ground-state energy of an interacting Bose gas with a purely repulsive potential. It consists in the derivation of an equation, which is not based on perturbation theory and which gives the exact expansion of the energy at low densities. This equation is expressed directly in the thermodynamic limit and only involves functions of three variables, rather than $3N$. Here, we revisit this approach, introduce two more equations, and show that these yields accurate predictions for various observables for *all* densities for repulsive potentials with positive Fourier transform. Specifically, in addition to the ground-state energy, we have shown that the simplified approach gives predictions for the condensate fraction, two-point correlation function, and momentum distribution. We have carried out a variety of tests by comparing the predictions of the equations with quantum Monte Carlo calculations for exponential interaction potentials as well as a different, finite range potential of positive type, and have found remarkable agreement. We thus show that the simplified approach provides an alternative theoretical tool to understand the behavior of the many-body Bose gas, not only in the small and large density ranges, which have been studied before, but also in the range of intermediate density, for which much less is known.

DOI: 10.1103/PhysRevA.103.053309

I. INTRODUCTION

Bose gases are one of the foundational objects in the statistical mechanics of quantum systems, and have been the focus of much scrutiny, dating back to the early days of quantum mechanics [1]. Nevertheless, there are still several important problems to be solved, in the case of interacting Bose gases, in which the correlations between particles make the analysis very difficult. In this case, observables may be computed by either performing numerical computations using finite-size approximations and extrapolations, or by devising effective theories which capture some of the correlations between particles, while remaining integrable. In this paper, we present an effective theory which goes back to 1963 [2], and which we have found gives accurate predictions in the thermodynamic limit at *all* densities that have been verified numerically by quantum Monte Carlo (QMC) computations. This remarkable agreement leads us to suggest that this may be a new way of understanding and analyzing the quantum many-body problem.

In the low density regime, an effective theory which has proved to be extremely successful is due to Bogolubov [3], who devised a scheme in which the many body-Hamiltonian is reduced to a quadratic operator, which captures pair correlations rather well, and, at the same time, can be explicitly diagonalized (see Ref. [4] for a review). By applying Bogolubov's scheme to an idealized Hamiltonian in which the interaction potential v is replaced by a localized *pseudopotential*, Lee, Huang and Yang derived a large collection of predictions for the Bose gas at low density. In particular, they computed that the ground-state energy per particle should behave as [5, (25)]

$$e_0 = 2\pi\rho a_0\left(1 + \frac{128}{15\sqrt{\pi}}\sqrt{\rho a_0^3}\right), \tag{1}$$

where ρ is the particle density, a_0 is the scattering length of v (throughout this paper, we will take $\hbar = m = 1$). The leading order term $2\pi\rho a_0$ is originally due to Lenz [1]. The Lee-Huang-Yang formula (1) can also be derived from the computation done by Bogolubov [3,6]. This expansion is *universal*, in that it only depends on the scattering length a_0, and not on the details of the potential. Lee, Huang, and Yang also made a prediction for the ground-state noncondensed fraction η_0, that is, the fraction of particles that are *not* in the Bose-Einstein condensate [5, (41)]:

$$\eta_0 = \frac{8\sqrt{\rho a_0^3}}{3\sqrt{\pi}}. \tag{2}$$

After much work over more than sixty years, it was finally proved [7–14] that (1) is asymptotically correct at low densities. The formula for the noncondensed fraction (2) has, to

*carlen@rutgers.edu
†markus.holzmann@grenoble.cnrs.fr
‡ijauslin@princeton.edu
§lieb@princeton.edu

 ©2021 American Physical Society

this day, not been proved to hold for the interacting Bose gas in the thermodynamic limit, though it has been confirmed by numerical experiments [15].

Concerning the ground-state energy at high densities, it has been shown [2] that if the potential is of positive type (non-negative with a non-negative Fourier transform), then, as $\rho \to \infty$,

$$e_0 \sim \frac{\rho}{2} \int d\mathbf{x}\, v(\mathbf{x}). \tag{3}$$

The positivity of the Fourier transform of the potential is required for this to hold. In fact, Sütő [16] has proved that, for the classical Bose gas (at asymptotically large densities, for many potentials, the classical ground state coincides with the quantum one), the high-density ground state is uniform for positive type potentials, but it exhibits periodic patterns for certain potentials that are not of positive type. In the latter case, (3) cannot possibly hold. In Sec. V, we will discuss a simple example of a potential that is not of positive type for which $e_0/\rho \to 0$. From now on, we will restrict our attention to potentials of positive type. The asymptotic formula (3) coincides with the ground-state energy in Hartree theory, in which all Bosons are assumed to be condensed. Note that, whereas Hartree theory is accurate at asymptotically large densities, there are various effective theories that produce accurate results for large finite densities, such as those based on the random phase approximation and the mean spherical approximation (MSA) [17].

Therefore the Bose gas is described by Bogolubov theory at low density and Hartree theory or the MSA at high density. In this paper, we will discuss another effective theory for the ground state of the repulsive Bose gas with a positive type potential, which is highly accurate at all densities, which is *exact* at low and high densities, and highly accurate at all intermediate densities. In other words, it is a physically descriptive interpolation between Bogolubov and Hartree theory. To justify our claim that it is in good *quantitative* agreement with the physics at all densities, we rely on with QMC simulations of the Bose gas for intermediate densities. This equation was originally introduced in 1963 [2] and studied for the high density jellium [18] and in one dimension [19]. There has been no research progress since then. The merit of this equation is twofold. First, it provides a tool to study the Bose gas at intermediate densities, about which little is known, and, since the Bose gas is strongly correlated in this regime, we expect the physical behavior of the system to be significantly different from the low and high density limits. Second, the approach leading to this equation is quite different from Bogolubov theory, so it may shine a new light on the low density physics of the system, and, perhaps, lead to progress in the proof of the existence of Bose-Einstein condensates at small positive densities. The effective theory described in this paper gives a prediction for a function derived from the ground-state wave function ψ_0 of the Bose gas in the thermodynamic limit, which is automatically symmetric and non-negative:

$$g_2(\mathbf{x}_1 - \mathbf{x}_2) := \lim_{\substack{N,V\to\infty \\ \frac{N}{V}=\rho}} \frac{\int \frac{d\mathbf{x}_3}{V} \cdots \frac{d\mathbf{x}_N}{V}\, \psi_0(\mathbf{x}_1, \mathbf{x}_2, \cdots, \mathbf{x}_N)}{\int \frac{d\mathbf{y}_1}{V} \cdots \frac{d\mathbf{y}_N}{V}\, \psi_0(\mathbf{y}_1, \cdots, \mathbf{y}_N)}. \tag{4}$$

The function g_2 can be interpreted as the two-point correlation function of the probability distribution $\psi_0 \geqslant 0$ (suitably normalized). Note that this is different from the quantum probability distribution $|\psi_0|^2$. The effective theory gives a prediction, denoted by u, for an approximation of $1 - g_2(\mathbf{x} - \mathbf{y})$. This prediction satisfies the following equation [2]:

$$[-\Delta + v(\mathbf{x})]u(\mathbf{x}) = v(\mathbf{x}) - \rho[1 - u(\mathbf{x})][2K(\mathbf{x}) - \rho L(\mathbf{x})] \tag{5}$$

with

$$K(\mathbf{x}) := \int d\mathbf{y}\, u(\mathbf{y} - \mathbf{x})S(\mathbf{y}) \equiv u * S(\mathbf{x}), \tag{6}$$

$$S(\mathbf{x}) := (1 - u(\mathbf{x}))v(\mathbf{x}), \tag{7}$$

$$L(\mathbf{x}) := \int d\mathbf{y}d\mathbf{z}\, u(\mathbf{y})u(\mathbf{z} - \mathbf{x})\Big(1 - u(\mathbf{z}) - u(\mathbf{y} - \mathbf{x}) + \frac{1}{2}u(\mathbf{z})u(\mathbf{y} - \mathbf{x})\Big)S(\mathbf{z} - \mathbf{y}). \tag{8}$$

This equation will be called the full equation, as we will also be considering a hierarchy of three approximations to this equation.

(1) The big equation (which will be rendered in plots in **yellow**), in which we neglect the $\frac{1}{2}u(\mathbf{z})u(\mathbf{y} - \mathbf{x})$ term in (8):

$$-\Delta u(\mathbf{x}) = (1 - u(\mathbf{x}))(v(\mathbf{x}) - 2\rho K(\mathbf{x}) + \rho^2 L_{\text{bigeq}}(\mathbf{x})) \tag{9}$$

with

$$L_{\text{bigeq}} := u * u * S - 2u * (u(u * S)). \tag{10}$$

(2) The medium equation (**green**), in which we further neglect the $2u * (u(u * S))$ term in (10), and drop the $u(\mathbf{x})$ in the $(1 - u(\mathbf{x}))$ prefactor of K and L_{bigeq} in (9):

$$-\Delta u(\mathbf{x}) = (1 - u(\mathbf{x}))v(\mathbf{x}) - 2\rho K(\mathbf{x}) + \rho^2 L_{\text{mueq}}(\mathbf{x}) \tag{11}$$

with

$$L_{\text{mueq}} := u * u * S. \tag{12}$$

(3) The simple equation (**blue**), in which we further approximate S by $\delta(\mathbf{x})\frac{2\tilde{e}}{\rho}$ in (6) and (12):

$$(-\Delta + v(\mathbf{x}) + 4\tilde{e})u(\mathbf{x}) = v(\mathbf{x}) + 2\tilde{e}\rho u * u(\mathbf{x}) \tag{13}$$

with

$$\tilde{e} = \frac{\rho}{2} \int d\mathbf{x}\, (1 - u(\mathbf{x}))v(\mathbf{x}). \tag{14}$$

The basis for making these approximations is discussed in Sec. II. The big equation is easier to solve numerically than the full equation, yet it remains very accurate. However, the mathematical analysis of the full, big, and medium equations is quite difficult and so far has not been accomplished. In this regard, the situation is much better for the simple equation, for which a well-developed mathematical study has been carried out in Refs. [20,21], and it is also quite simple to investigate its solutions numerically. The medium equation also has this latter advantage; it has a simpler structure than the big equation and is considerably easier to solve numerically. As we show here it gives good results over a wider range of densities than the simple equation.

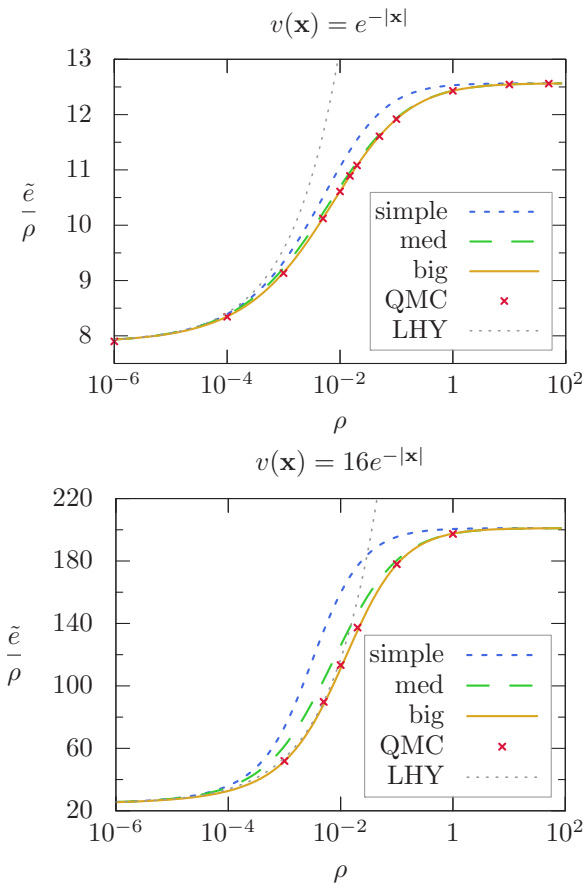

FIG. 1. The energy as a function of density for the potential $e^{-|\mathbf{x}|}$ (top) and $16e^{-|\mathbf{x}|}$ (bottom). We compare the predictions of the big, medium, and simple equations to a QMC simulation. For comparison, we also plot the Lee-Huang-Yang (LHY) energy (1). (All quantities plotted in this and the following figures are dimensionless).

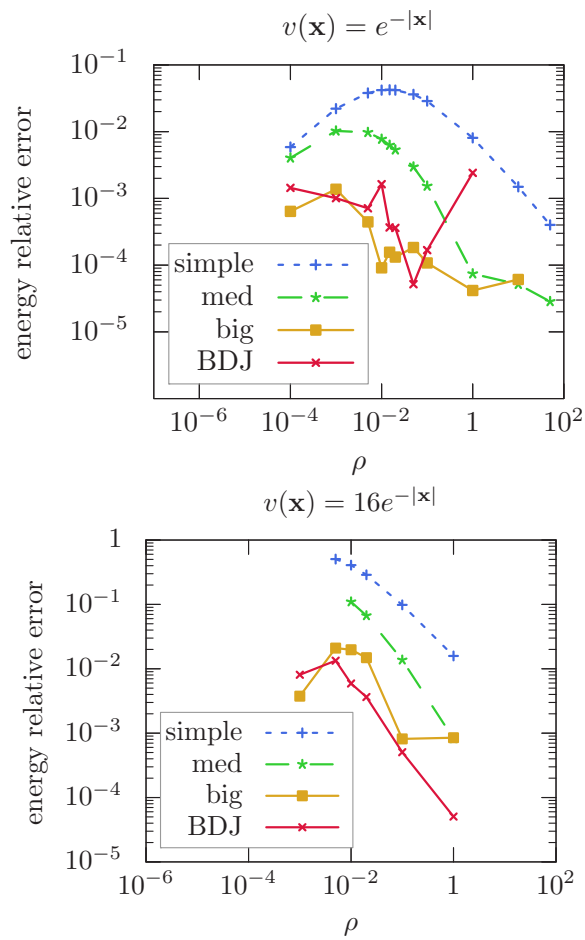

FIG. 2. Relative error for the energy $\frac{\tilde{e}-e_{\mathrm{QMC}}}{e_{\mathrm{QMC}}}$ compared to the QMC simulation as a function of density for the potential $e^{-|\mathbf{x}|}$ (top) and $16e^{-|\mathbf{x}|}$ (bottom). The red crosses are the result for the optimal Bijl-Dingle-Jastrow (BDJ) function.

The simple equation nonetheless gives accurate results at least for low and high densities, for which it yields asymptotically correct results. In a previous publication [20], we proved that the simple equation predicts an energy that coincides asymptotically with (1) at low density, and with (3) at high density. In another paper [21], released concurrently with the present paper, we prove that the condensate fraction predicted by the simple equation agrees asymptotically with (2) at low density.

In the present paper, we discuss some more quantitative results, with more of a focus on the big equation, which we have found to be very accurate by comparing its predictions to quantum Monte Carlo simulations. We will consider potentials that are of positive type, with a special focus on exponential potentials of the form $\alpha e^{-|\mathbf{x}|}$. We have found that the prediction for the energy is very accurate for *all* densities, see Fig. 1. In the case $\alpha = 1$, the relative error compared to the QMC simulation is as small as 0.1%, and is comparable to the error made by a Bijl-Dingle-Jastrow function ansatz [22–24], see Fig. 2, even though the solution of the big equation is much easier to compute numerically than the Bijl-Dingle-Jastrow optimizer. The prediction for the condensate fraction is less accurate in the intermediate density regime, though still remarkably good for small values of α, see Fig. 3. For larger α, the big equation is off the mark, see Fig. 9, although the qualitative features of the condensate fraction are still well

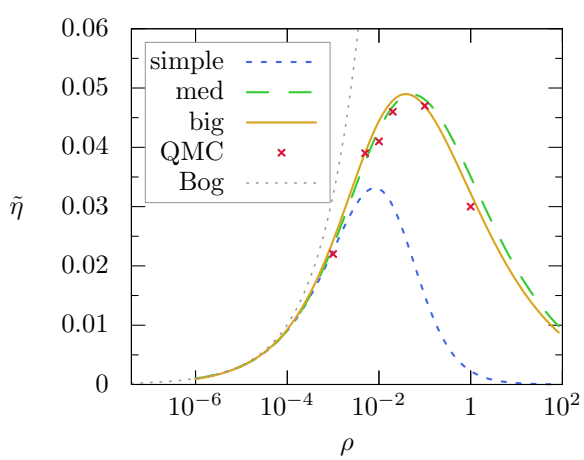

FIG. 3. The noncondensed fraction as a function of the density for the potential $\frac{1}{2}e^{-|\mathbf{x}|}$. We compare the predictions of the big, medium, and simple equations to a QMC simulation. The prediction of Bogolubov theory (2) is also plotted for comparison (Bog).

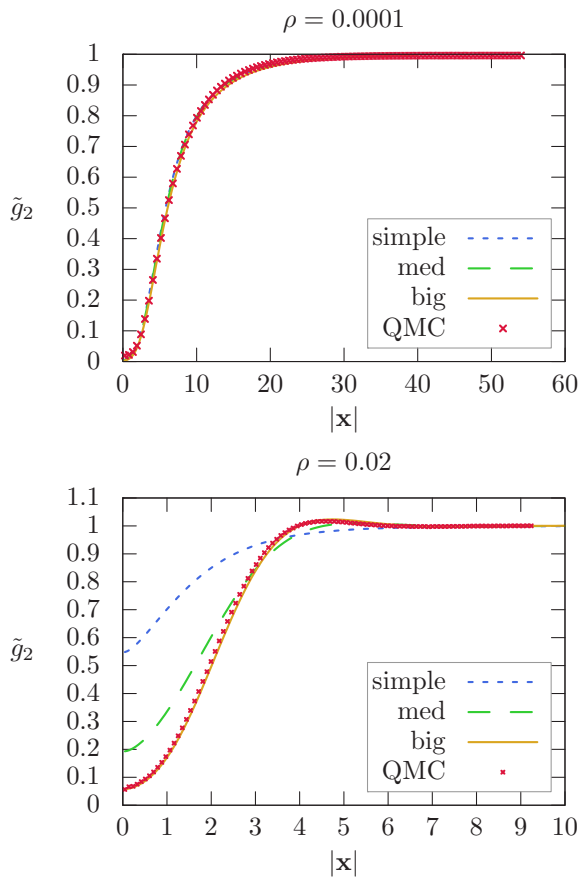

FIG. 4. $\tilde{g}_2(\mathbf{x})$ for the potential $16e^{-|\mathbf{x}|}$ at $\rho = 0.0001$ (top) and $\rho = 0.02$ (bottom). We compare the predictions of the big, medium, and simple equations to a QMC simulation.

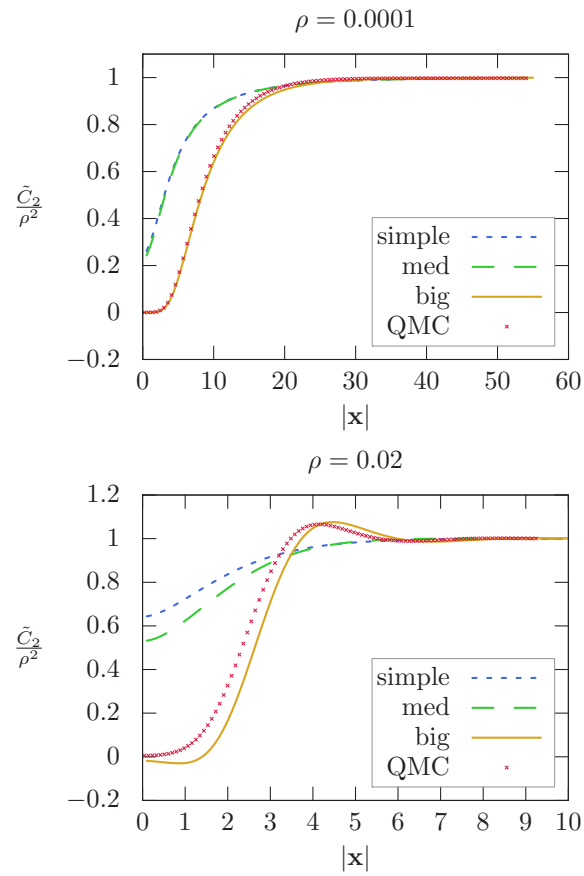

FIG. 5. $\frac{\tilde{C}_2}{\rho^2}$ for the potential $e^{-|\mathbf{x}|}$ at $\rho = 0.0001$ (top) and $\rho = 0.02$ (bottom). We compare the predictions of the big, medium, and simple equations to a QMC simulation.

reproduced. We have also carried out similar computations for the hard core potential, for which we also find good agreement, see Fig. 8.

Because computing with the big equation is relatively easy from a computational point of view, we have been able to probe some observables in the intermediate density regime, far from the low density Bogolubov regime and the high density mean field regime. Comparing to QMC simulations, we have found that g_2 [see Eq. (4)] is accurately predicted by both the simple and the big equations at low density, but, as the density is increased, the prediction from the simple equation drops away abruptly, but the big equation remains accurate: see Fig. 4. When this occurs, a maximum that is >1 appears, thus indicating that there is a new length scale appearing in the problem, at which there is a small increase in the probability of finding a particle. This picture also holds for the usual quantum two-point correlation function, which we can also predict rather accurately, see Fig. 5. This suggests a nontrivial, strongly coupled phase at intermediate densities, which was thus predicted by the big equation and validated by QMC simulations. Naturally, this is not the first investigation into strongly coupled Bose gases. Indeed, there has been much interest lately in the *unitary Bose gas*, in which case the interaction potential is a Dirac delta function (a contact interaction), and the scattering length is taken to infinity (see Ref. [25] for a review). Increasing the scattering length results in nontrivial many-particle effects, such as the appearance of Efimov trimers [26–28]. This can be seen [29–33] in terms of the *universal* Tan relation [34], which states that the momentum distribution $\mathcal{M}(\mathbf{k})$ satisfies, at large $\mathbf{k}$,

$$\mathcal{M}_0(\mathbf{k}) \sim \frac{c_2}{|\mathbf{k}|^4}, \quad c_2 = 8\pi a_0^2 \frac{\partial e_0}{\partial a_0}. \tag{15}$$

For the big and simple equations discussed in this paper, we have found that this relation holds in the range

$$\sqrt{\rho a_0} \ll |\mathbf{k}| \ll 1 \tag{16}$$

which is another confirmation of the accuracy of the effective equation at small densities. However, if $\sqrt{\rho} \gtrsim 1$, then the universal Tan regime does not exist, and the picture in terms of strongly coupled few-particle configurations inherent to the analysis of unitary Bose gases [29,31] breaks down, as the Bose gas transitions to a strongly correlated liquid. This is confirmed for the prediction of the big equation, see Fig. 6.

As further evidence of the breakdown of universality in the intermediate density regime, we have also compared the ground-state energy for two very different potentials, which have the same scattering length and the same integral. We have found that the energy for these two potentials is significantly different in the intermediate density regime, see Fig. 7. For

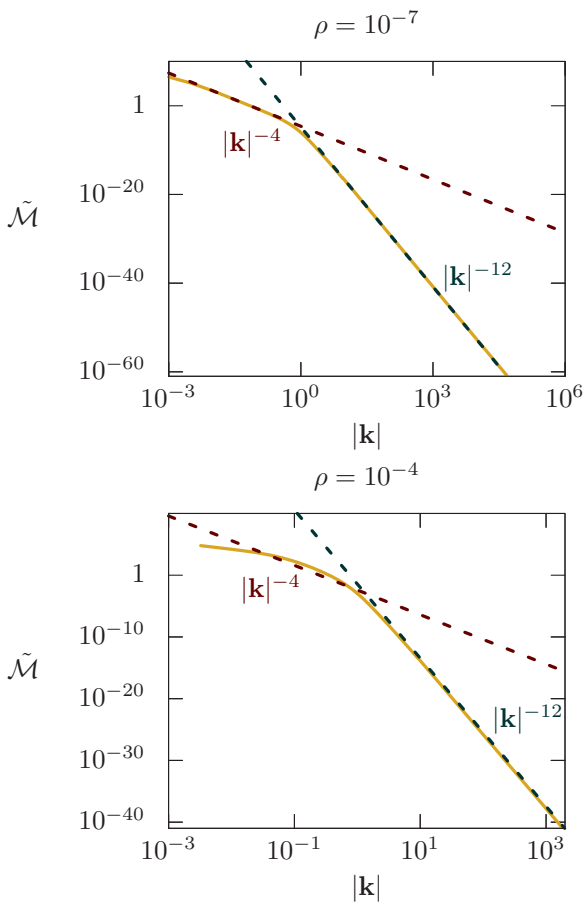

FIG. 6. The prediction of the big equation for the momentum distribution as a function of $|\mathbf{k}|$ for the potential $e^{-|\mathbf{x}|}$, $\rho = 10^{-7}$ (top) and $\rho = 10^{-4}$ (bottom). The dark red dotted line has a slope of -4 and corresponds to a $|\mathbf{k}|^{-4}$ behavior, whereas the dark green dotted line has a slope -12, and corresponds to $|\mathbf{k}|^{-12}$.

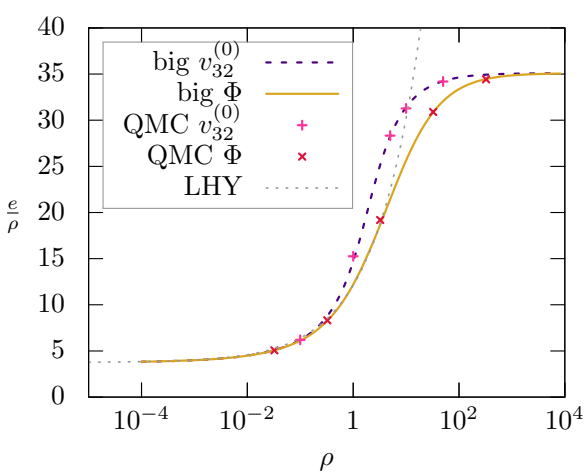

FIG. 7. The prediction of the energy by the big equation for the potentials $v_{32}^{(0)}$ and $\Phi(\mathbf{x}) \equiv \alpha e^{-\beta|\mathbf{x}|}$ with $\alpha \approx 907.2$ and $\beta \approx 6.873$. The potentials are chosen to have the same scattering length, $a_0 \approx 0.5878$, as well as the same value for their integrals, so they coincide at low and at high densities. They differ signinficantly at intermediate densities. We compare each curve to a few QMC points, which fit well. We also plot the Lee-Huang-Yang (LHY) energy (1).

these two potentials, we have also found that the quantum Monte Carlo data fits very well with the prediction of the big equation. The rest of the paper is structured as follows. In Sec. II, we detail the approximation needed to get from the many-body Bose gas to the full fquation, and then discuss the approximations leading to the big, medium, and simple equations. In Sec. III, we compare various physical quantities predicted by these equations to QMC simulations of the Bose gas. In Sec. IV, we treat the hard core potential. In Sec. V, we discuss the limitations of the approximations.

II. DERIVATION OF THE FULL EQUATION AND ITS APPROXIMATIONS

Let us now discuss the derivation of the full equation, which follows [2], and the approximations that lead to the big, medium, and simple equations. Whereas this derivation is based on uncontrolled approximations, it is justified by the remarkable accuracy of the resulting predictions compared to QMC computations. We start from the many-body Hamiltonian: denoting the number of particles by N,

$$H = -\frac{1}{2}\sum_{i=1}^{N}\Delta_i + \sum_{1\leqslant i<j\leqslant N} v(\mathbf{x}_i - \mathbf{x}_j) \tag{17}$$

(we set $\hbar = m = 1$). We confine the N particles in a cubic box Λ of volume V, and impose periodic boundary conditions. Later on, we will take the thermodynamic limit $N, V \to \infty$, $\frac{N}{V} = \rho$ fixed.

In the derivation presented here, we will rely on the translation invariance of the Hamiltonian, which does not allow us to study a system with a trapping potential at this time.

Let E_N denote the ground-state energy and let $\psi_N(\mathbf{x}_1, \ldots, \mathbf{x}_N)$ denote the ground-state wave function so that

$$H\psi_0(\mathbf{x}_1, \ldots, \mathbf{x}_N) = E_N\psi_N(\mathbf{x}_1, \ldots, \mathbf{x}_N), \tag{18}$$

where $v \geqslant 0$ is an integrable pair potential. Instead of taking the scalar product of both sides of the equation with ψ_0, which would yield an expression relating the ground-state energy to the one-particle reduced density matrix, we will simply integrate both sides of the equation, and find that, using the translation invariance of the system,

$$\frac{E_N}{N} = \frac{N-1}{2V}\int d\mathbf{x}\, v(\mathbf{x}) g_2^{(N)}(\mathbf{x}) \tag{19}$$

with

$$g_n^{(N)}(\mathbf{x}_2 - \mathbf{x}_1, \ldots, \mathbf{x}_N - \mathbf{x}_1) := \frac{\int \frac{d\mathbf{x}_{n+1}}{V}\cdots\frac{d\mathbf{x}_N}{V}\,\psi_0(\mathbf{x}_1, \cdots, \mathbf{x}_N)}{\int \frac{d\mathbf{x}_1}{V}\cdots\frac{d\mathbf{x}_N}{V}\,\psi_0(\mathbf{x}_1, \cdots, \mathbf{x}_N)}. \tag{20}$$

In particular, note that the kinetic term has disappeared entirely. Furthermore, by the Perron-Frobenius theorem, $\psi_0 \geqslant 0$, so $g_n^{(N)}$ can be interpreted as the n-point correlation function of the probability distribution ψ_0 (suitably normalized) which is not the usual quantum probability distribution.

We can then express $g_2^{(N)}$ by integrating (18) with respect to $\mathbf{x}_3, \ldots, \mathbf{x}_N$: using the translation invariance of the system,

$$-\Delta g_2^{(N)}(\mathbf{x}-\mathbf{y}) + v(\mathbf{x}-\mathbf{y})g_2^{(N)}(\mathbf{x}-\mathbf{y}) + \frac{N-2}{V}\int d\mathbf{z}\,(v(\mathbf{x}-\mathbf{z}) + v(\mathbf{y}-\mathbf{z}))g_3^{(N)}(\mathbf{y}-\mathbf{x}, \mathbf{z}-\mathbf{x}) + \frac{(N-2)(N-3)}{2V^2}$$
$$\times \int d\mathbf{z}dt\; v(\mathbf{z}-t)g_4^{(N)}(\mathbf{y}-\mathbf{x}, \mathbf{z}-\mathbf{x}, t-\mathbf{x}) = E_0 g_2^{(N)}(\mathbf{x}-\mathbf{y}). \tag{21}$$

This equation relates g_2 to g_3 and g_4. By proceeding in the same way, we can derive equations for g_3 and g_4 in terms of g_5 and g_6, and so on. In this way, we obtain a hierarchy of equations for all the $g_n^{(N)}$.

The full equation is an approximation in which we truncate this hierarchy at the lowest level, by assuming that g_3 and g_4 can be expressed in terms of g_2, which turns (21) into an equation for $g_2^{(N)}$ alone. Remembering that g_n can be interpreted as a correlation function, it is natural to approximate g_3 and g_4 by

$$g_3^{(N)}(\mathbf{x}_2-\mathbf{x}_1, \mathbf{x}_3-\mathbf{x}_1) = g_2^{(N)}(\mathbf{x}_2-\mathbf{x}_1)g_2^{(N)}(\mathbf{x}_3-\mathbf{x}_1)g_2^{(N)} \times (\mathbf{x}_3-\mathbf{x}_2) \tag{22}$$

and

$$g_4^{(N)}(\mathbf{x}_2-\mathbf{x}_1, \mathbf{x}_3-\mathbf{x}_1, \mathbf{x}_4-\mathbf{x}_1) = \prod_{i<j}\left(g_2^{(N)}(\mathbf{x}_j-\mathbf{x}_i) + R(\mathbf{x}_j-\mathbf{x}_i)\right) \tag{23}$$

in which the correction term $R(\mathbf{x}_j-\mathbf{x}_i) = O(V^{-1})$ is relevant because $g_4^{(N)}$ appears in (21) in a term that diverges as V in the thermodynamic limit. This correction term is computed by ensuring that $\int d\mathbf{x}_3 d\mathbf{x}_4\, g_4^{(N)} = V^2 g_2^{(N)}$:

$$R(\mathbf{x}-\mathbf{y}) = -\frac{2}{V}g_2^{(N)}(\mathbf{x}-\mathbf{y})\int d\mathbf{z}\left(1-g_2^{(N)}(\mathbf{z}-\mathbf{x})\right) \times \left(1-g_2^{(N)}(\mathbf{z}-\mathbf{y})\right) + O(V^{-2}). \tag{24}$$

Taking the thermodynamic limit $N, V \to \infty$, $\frac{N}{V} = \rho$, we find (5) by defining

$$g_2(\mathbf{x}) =: 1 - u(\mathbf{x}). \tag{25}$$

Furthermore, by (19), the prediction for the ground-state energy is

$$\tilde{e} = \frac{\rho}{2}\int d\mathbf{x}\,(1-u(\mathbf{x}))v(\mathbf{x}). \tag{26}$$

The factorization assumption (22)-(23) simply states that many-body correlations of ψ_0 reduce to pair correlations. If ψ_0 were Gaussian, this would hold exactly. If ψ_0 were a Bijl-Dingle-Jastrow function [22–24], that is, if

$$\psi_0 = \prod_{i<j} e^{-\beta\varphi(\mathbf{x}_i-\mathbf{x}_j)} \tag{27}$$

then the factorization property at long distances would be equivalent to the fact that the classical statistical mechanical model with interaction φ satisfies the *clustering property* [35]. One can expect this to be true at low densities, where the Bijl-Dingle-Jastrow function might be a good approximation of the ground state. At high densities, since the system approaches a mean-field regime, one might also suppose that the factorization assumption may not be so far off.

The full equation we have derived is quite difficult to study, even numerically. As was discussed in Sec. I, we will introduce further approximations to simplify the equation. The first approximation is to neglect the $\frac{1}{2}u(\mathbf{z})u(\mathbf{y}-\mathbf{x})$ term in (8), which is the most difficult term, from a computational point of view. We expect that, at low densities, this term is expected to be of order $\rho^{3/2}$ uniformly in $\mathbf{x}$, whereas the leading order term in L should be of order ρ. This leads us to the big equation defined in (9). This equation is easier to solve numerically than the full equation, because in Fourier space, it involves only two convolution operators, whereas the full equation contains three, which makes it computationally heavier. Nevertheless, this equation is still difficult to study analytically, so we make further approximations

Following the same idea, we can further neglect the $2u * (u(u * S))$ term in (10). Furthermore, we expect u to decay as $|\mathbf{x}|^{-4}$, so if we focus on distances that are appreciably large, we can approximate $1-u$ by 1 in the prefactor of K and L in (9). This leads to the Medium Eq. (11).

To arrive at the simple equation, we take advantage of a separation of scales that occurs at low density. On account of (19), the function $S(\mathbf{x})$ defined in (6) satisfies

$$\int d\mathbf{x}\, S(\mathbf{x}) = \frac{2\tilde{e}}{\rho} \tag{28}$$

which is just another way of stating (26). There are two different length scales in the problem: the first is the scattering length of the potential a_0 and the second is the interparticle distance $\rho^{-1/3}$. At sufficiently low densities, we will have

$$a_0 \ll \rho^{-1/3} \tag{29}$$

and if the length scale $\rho^{-1/3}$ is characteristic of the solution u of (5), as we argue below, then we can expect $u(\mathbf{x})$ to satisfy a bound of the form $|\nabla u(\mathbf{x})| \leqslant C\rho^{1/3}$ uniformly in $\mathbf{x}$. When integrating $S(\mathbf{x})$ against such a slowly varying function, we may as well replace it with $2\tilde{e}/\rho$ times a delta function:

$$S(\mathbf{x}) \approx \frac{2\tilde{e}}{\rho}\delta(\mathbf{x}). \tag{30}$$

Making this approximation in (6) and (12), we arrive at the simple Eq. (13). Notice the energy per particle $\tilde{e}$ appears as an explicit parameter in the simple equation, unlike the full equation.

III. COMPARISON WITH QUANTUM MONTE CARLO SIMULATIONS

Exact ground-state properties of finite N-boson systems can be calculated arbitrarily well numerically with QMC

methods. At zero temperatures, it is convenient to first introduce a trial wave function, ψ_{trial}, containing parameters which are numerically optimized by minimizing the corresponding variation energy evaluated by variational Monte Carlo (VMC) calculations [36]. Subsequently, the exact ground-state wave function ψ_0 is accessed stochastically by imaginary time projection [37–39].

Here, we have performed ground-state QMC calculations for N bosons in a periodic box interacting with an exponential potential, $\alpha e^{-|\mathbf{x}|}$. Our calculations are based on a pair-product (Bijl-Dingle-Jastrow) trial wave function, $\psi_{\text{trial}} \propto \exp(-\sum_{i<j} \varphi(|\mathbf{x}_i - \mathbf{x}_j|))$, where φ is parametrized via locally piecewise-quintic Hermite interpolants in real space and Fourier coefficients in reciprocal space.

In variational Monte Carlo, ψ^2_{trial} is sampled by Metropolis Monte Carlo, and the optimal variational parameters of φ are determined by minimizing a linear combination of the energy and its variance. Using the optimized ψ_{trial} as a guiding function, the mixed distribution $\psi_0\psi_{\text{trial}}$ is then stochastically sampled by diffusion Monte Carlo (DMC). Linear extrapolation is used to reduce the mixed-estimator bias occurring for observables different from the ground-state energy [40]. In principle, the mixed-estimator bias can be controlled either by systematic improvement of the trial wave function [41] or by different projection Monte Carlo methods, e.g., reptation Monte Carlo [39]. For the system under consideration, the mixed estimator bias of the pair-product wave function was found to be sufficiently small, the overall precision being limited rather by the finite system size of the QMC calculations.

In contrast to the computation of the big, medium, and simple equations, QMC calculations require an explicit numerical extrapolation from finite to infinite system size, which is frequently one of the main bottlenecks of the method. Finite size errors in the kinetic and potential energy can be quantified based on two-body correlation functions [42]. In addition, we have performed VMC and DMC calculations for various system sizes, ranging from $N = 8$ to 512 bosons, to accurately extrapolate to the thermodynamic limit.

In the figures, errors of the QMC calculations are smaller than the size of the crosses in the plots, see Fig. 1. QMC results for hard core Bosons are taken from Ref. [15].

A. Energy

Of the observables considered in this paper, the ground-state energy is the most straightforward to compute: by (26), the prediction for the energy is

$$\tilde{e} = \int d\mathbf{x}\,(1 - u(\mathbf{x}))v(\mathbf{x}). \tag{31}$$

In our notation, e_0 is the ground-state energy per particle for the exact ground state of the Bose gas, and $\tilde{e}$ is the prediction for the ground-state energy by the big, medium, or simple equation.

In Fig. 1, we show a comparison of the prediction $\tilde{e}$ with a QMC simulation for the exponential potential $\alpha e^{-|\mathbf{x}|}$. In Ref. [20], we proved that the energy prediction of the simple equation is asymptotically correct in both the low and high density limits. The numerics confirm this for all three equations. For $\alpha = 1$, the simple equation is somewhat accurate, although the Medium and big equations are much closer to the QMC simulation. For $\alpha = 16$ this is even clearer, and one sees that the Medium equation is more accurate at large densities than at small ones.

A more quantitative comparison can be found in Fig. 2, where we plot the relative error, that is, $(\tilde{e} - e_{\text{QMC}})/e_{\text{QMC}}$, where e_{QMC} is the quantum Monte Carlo prediction for the energy. We find that, for $\alpha = 1$, the relative error is, at most, 5% for the simple equation, 1% for the Medium equation, and 0.1% for the big equation. For $\alpha = 16$, all equations are less accurate, with a relative error of 60% for the simple equation, 10% for the Medium equation, and 2% for the big equation.

In addition, in Fig. 2, we compare with the error made by the optimal Bijl-Dingle-Jastrow function. A Bijl-Dingle-Jastrow function is an ansatz for the ground-state wave function of the form (27). Finding the optimal function φ which minimizes the energy is a computationally intensive operation, which is used as a first approximation when running the diffusion QMC simulation used in Fig. 1. We find that the optimal Bijl-Dingle-Jastrow function gives a prediction for the ground-state energy which is about as accurate as the big equation. Of note is the fact that solving the big equation numerically is computationally much less difficult than computing the optimal Bijl-Dingle-Jastrow function. In addition, in Fig. 2, we see that the full equation and the big equation produce very similar results.

B. Condensate fraction

The approximations leading to the Big, Simple and Medium equations reduce the number of degrees of freedom from $3N$ in the many body Bose gas to just 3. In doing so, we lose some information, and, in particular, we do not obtain a prediction for the many-body wave function ψ_0. Therefore computing observables other than the ground-state energy is not entirely straightforward. To compute the condensate fraction, we first express it in terms of the energy of an auxiliary system, from which we derive an approximation following the prescriptions in Sec. II. Specifically, the noncondensed fraction of the many-body ground state ψ_0

$$\eta_0 := 1 - \frac{1}{N}\sum_{i=1}^{N}\langle\psi_0|P_i|\psi_0\rangle \tag{32}$$

is expressed in terms of the projector $P_i\psi_0 := \int \frac{d\mathbf{x}_i}{V}\psi_0$ onto the condensate wave function (which is the constant function): which we re-express in terms of the modified Hamiltonian

$$H_\mu = -\frac{1}{2}\sum_{i=1}^{N}\Delta_i + \sum_{1\leqslant i<j\leqslant N} v(\mathbf{x}_i - \mathbf{x}_j) - \mu\frac{1}{N}\sum_{i=1}^{N}P_i, \tag{33}$$

whose ground-state energy per particle is denoted by $e_{0,\mu}$:

$$\eta_0 = 1 + \partial_\mu e_{0,\mu}\big|_{\mu=0}. \tag{34}$$

Following the approximation scheme in Sec. II, we compute an approximation $\tilde{e}_\mu$ for $e_{0,\mu}$ (following the convention used before, $e_{0,\mu}$ is the energy for the exact many-body ground state and $\tilde{e}_\mu$ is the prediction of the big, medium, and simple

equations):

$$(-\Delta + 2\mu)u_\mu(\mathbf{x}) = (1 - u_\mu(\mathbf{x}))(v(\mathbf{x}) - 2\rho K(\mathbf{x}) + \rho^2 L(\mathbf{x})) \tag{35}$$

$$\tilde{e}_\mu = \int d\mathbf{x}\,(1 - u_\mu(\mathbf{x}))v(\mathbf{x}) \tag{36}$$

[compare this to (5)]. This leads to an approximation $\tilde{\eta}$ for the noncondensed fraction η_0:

$$\tilde{\eta} := 1 + \partial_\mu \tilde{e}_\mu\big|_{\mu=0}. \tag{37}$$

Proceeding as in Sec. II, we obtain predictions for the big, simple, and Medium equations.

In the case of the simple equation, we can relate $\tilde{\eta}$ and the solution u of the Eq. (13) directly:

$$\tilde{\eta} = \frac{\int d\mathbf{x}\, v(\mathbf{x})\mathfrak{K}_{\tilde{e}}u(\mathbf{x})}{1 - \rho \int d\mathbf{x}\, v(\mathbf{x})\mathfrak{K}_{\tilde{e}}(2u(\mathbf{x}) - \rho u * u(\mathbf{x}))}, \tag{38}$$

where $\mathfrak{K}_{\tilde{e}}$ is the operator

$$\mathfrak{K}_{\tilde{e}} := (-\Delta + 4\tilde{e}(1 - \rho u*) + v)^{-1}. \tag{39}$$

In Ref. [21], we study this operator in detail, and derived the low density limit of $\tilde{\eta}$:

$$\tilde{\eta} \underset{\rho\to 0}{\sim} \frac{8\sqrt{\rho a_0^3}}{3\sqrt{\pi}}, \tag{40}$$

which agrees with the prediction of Bogolubov theory (2) [5, (41)].

For the big and Medium equations, we carried out numerical computations, the results of which are reported in Fig. 3. Whereas all three approximate equations agree with one another very well at low densities, the simple equation becomes less accurate at intermediate densities. However, the big and Medium equations make rather accurate predictions (though not as accurate as for the energy), compared to the QMC simulation. We find, as expected, that all particles are condensed both at zero density and at infinite density, where the Bose gas becomes a mean-field system. The location of the maximum of the noncondensed fraction (or the minimum of the condensed fraction) is accurately predicted by the big and Medium equations.

C. Two-point correlation function

The two-point correlation function in the ground state is defined as

$$C_2(\mathbf{y} - \mathbf{y}') := \sum_{i,j=1}^{N} \langle \psi_0 | \delta(\mathbf{y} - \mathbf{x}_i)\delta(\mathbf{y}' - \mathbf{x}_j) | \psi_0 \rangle. \tag{41}$$

We first note that this can be rewritten in a way that makes the translation invariance of C_2 more apparent, by denoting $\mathbf{x} := \mathbf{y} - \mathbf{y}'$ and taking an average over $\mathbf{y}'$:

$$C_2(\mathbf{x}) := \frac{2}{V} \sum_{1\leqslant i<j\leqslant N} \langle \psi_0 | \delta(\mathbf{x} - (\mathbf{x}_i - \mathbf{x}_j)) | \psi_0 \rangle, \tag{42}$$

which we can rewrite as a functional derivative of the ground-state energy per particle e_0:

$$C_2(\mathbf{x}) = 2\rho^2 \frac{\delta e_0}{\delta v(\mathbf{x})}. \tag{43}$$

The prediction $\tilde{C}_2$ of the big and Medium equations for the two-point correlation function are therefore defined by differentiating $\tilde{e}$ in (26) with respect to v:

$$\tilde{C}_2(\mathbf{x}) := 2\rho^2 \frac{\delta \tilde{e}}{\delta v(\mathbf{x})}. \tag{44}$$

In the case of the simple equation, we will proceed differently. If we were to define $\tilde{C}_2$ as in (44), we would find that $\tilde{C}_2$ would not converge to ρ^2 as $|\mathbf{x}| \to \infty$, which is obviously unphysical. This comes from the fact that first approximating S as in (30) and then differentiating with respect to v is less accurate than first differentiating with respect to v and then approximating S. Defining $\tilde{C}_2$ following the latter prescription, we find that, for the simple equation,

$$\tilde{C}_2(\mathbf{x}) = \rho^2 \tilde{g}_2(\mathbf{x}) + \rho^2 \frac{\mathfrak{K}_{\tilde{e}}v(\mathbf{x})\tilde{g}_2(\mathbf{x}) - 2\rho u * \mathfrak{K}_{\tilde{e}}v(x) + \rho^2 u * u * \mathfrak{K}_{\tilde{e}}v(x)}{1 - \rho \int d\mathbf{x}\, v(\mathbf{x})\mathfrak{K}_{\tilde{e}}(2u(\mathbf{x}) - \rho u * u(\mathbf{x}))}, \tag{45}$$

where $\mathfrak{K}_{\tilde{e}}$ is the operator defined in (39). Defined in this way, $\tilde{C}_2 \to \rho^2$ as $|\mathbf{x}| \to \infty$.

C_2 is the physical correlation function, using the probability distribution $|\psi_0|^2$, but, as we saw in Sec. II, ψ_0 can also be thought of a probability distribution, whose two-point correlation function is g_2, defined in (20). The Big, Medium and simple equations make a natural prediction for the function g_2: namely $1 - u(\mathbf{x})$.

In Fig. 4, we compare the prediction $\tilde{g}_2$ produced by the big, medium, and simple equations to the QMC simulation. We find that for low enough densities, the three predictions are consistent with one another, and accurately reproduce the result of the QMC simulation. However, as the density is increased, there is a transition to a situation in which the predictions from the big, medium, and simple equations start to differ significantly from one another. In particular, in the case of the simple equation, $\tilde{g}_2 \leqslant 1$, whereas for the big and Medium equations, $\tilde{g}_2$ has a maximum that is >1. The prediction of the big equation remains quite accurate, when compared to the QMC simulation, which also exhibits a bump in g_2. The presence of this local maximum in g_2 shows that, in the probability distribution ψ_0, there is a larger probability of finding pairs of particles that are separated by a certain fixed distance. This indicates the appearance of a new physical length scale at intermediate densities, and indicates that the system exhibits a nontrivial physical behavior in this regime. Note that this behavior was observed for the stronger potential $16e^{-|\mathbf{x}|}$, but seems to be absent for $e^{-|\mathbf{x}|}$. Note, also, that, as will be discussed next, this maximum is also present in the two-point

correlation C_2, and is, therefore, the manifestation of a physical phenomenon.

In Fig. 5, we compare the prediction $\tilde{C}_2$ to the QMC simulation. At low densities, the prediction of the big equation agrees rather well with the QMC simulation. The Simple and Medium equations are not as accurate. At larger densities, the simple and Medium equations are quite far from the QMC computation, and the big equation is not as accurate as in the case of $\tilde{g}_2$, but it does reproduce some of the qualitative behavior of the QMC computation. In particular, there is a local maximum in the two-point correlation function, which occurs at a length scale that is close to that observed for $\tilde{g}_2$. This suggests the emergence of a nontrivial phase, which resembles a liquid. At small $\mathbf{x}$, $\tilde{C}_2$ is negative, which is clearly not physical, and those values should be discarded.

D. Momentum distribution

Next, we study the momentum distribution $\mathcal{M}_0(\mathbf{k})$. Computations carried out for the contact Hamiltonian [28,43] suggest that $\mathcal{M}_0$ should satisfy the asymptotic relation (15)

$$\mathcal{M}_0(\mathbf{k}) \sim \frac{c_2}{|\mathbf{k}|^4}, \quad c_2 = 8\pi a_0^2 \frac{\partial e_0}{\partial a} \tag{46}$$

and we will now discuss whether this holds for the big, simple, and Medium equations. To compute a prediction for the momentum distribution, we proceed in the same way as for the condensate fraction above. First of all, the momentum distribution is defined as

$$\mathcal{M}_0(\mathbf{k}) := \frac{1}{N}\sum_{i=1}^{N} \langle \psi_0 | F_i(\mathbf{k}) | \psi_0 \rangle \tag{47}$$

where F_i is the projection onto the state $e^{i\mathbf{k}\mathbf{x}_i}$. Thus, defining a modified Hamiltonian,

$$H_\lambda = -\frac{1}{2}\sum_{i=1}^{N} \Delta_i + \sum_{1\leqslant i<j\leqslant N} v(\mathbf{x}_i - \mathbf{x}_j) + \lambda \frac{1}{N}\sum_{i=1}^{N} F_i \tag{48}$$

whose ground-state energy per particle is denoted by $e_{0,\lambda}(\mathbf{k})$:

$$\mathcal{M}_0(\mathbf{k}) = \partial_\lambda e_{0,\lambda}(\mathbf{k})\big|_{\lambda=0}. \tag{49}$$

Proceeding as in Sec. II, this implies the following definition for the modified full equation [compare to Eq. (5)]: for $\mathbf{k} \neq 0$,

$$\begin{aligned}(-\Delta + v(\mathbf{x}))u_\lambda(\mathbf{x}) = v(\mathbf{x}) - \rho(1 - u_\lambda(\mathbf{x}))(2K(\mathbf{x}) - \rho L(\mathbf{x}))\\ - 2\lambda \hat{u}(\mathbf{k})\cos(\mathbf{k}\mathbf{x}),\end{aligned} \tag{50}$$

where $\hat{u}(\mathbf{k})$ is the Fourier transform of $u|_{\lambda=0}$, and

$$\tilde{e}_\lambda(\mathbf{k}) = \int d\mathbf{x}\, (1 - u_\lambda(\mathbf{x}))v(\mathbf{x}). \tag{51}$$

The prediction $\tilde{\mathcal{M}}$ for the momentum distribution $\mathcal{M}_0$ is then

$$\tilde{\mathcal{M}}(\mathbf{k}) := \partial_\lambda \tilde{e}_\lambda(\mathbf{k})\big|_{\lambda=0}. \tag{52}$$

We showed in Ref. [21] that, in the case of the simple equation, (15) holds in the limit in which $|\mathbf{k}|, \rho \to 0$ while $\frac{|\mathbf{k}|}{2\sqrt{\tilde{e}}} \to \infty$. This suggests that the Tan relation (15) only holds in the range

$$\sqrt{\rho} \ll |\mathbf{k}| \ll 1 \tag{53}$$

and, in particular, that if $\sqrt{\rho} \gtrsim 1$, then the Tan relation does not hold at all, which means that the physics of the Bose gas at intermediate densities is of a different nature from that studied in the context of the unitary Bose gas.

In Fig. 6, we show a numerical computation of $\tilde{\mathcal{M}}(\mathbf{k})$ for the big equation, at a very low density, and a larger one. As was predicted for the simple equation, we find that the Tan universal relation (15) holds at low density, provided $|\mathbf{k}|$ is small enough. At larger values of $|\mathbf{k}|$, the decay of $\hat{v}(\mathbf{k})$ kicks in, and the momentum distribution decays much faster. As the density is increased, the domain in which $\tilde{\mathcal{M}}(\mathbf{k}) \sim |\mathbf{k}|^{-4}$ shrinks to nothing, and the Tan universal relation completely disappears.

Here, we have not attempted a direct comparison of the momentum distribution with QMC calculations. From the previous comparisons of the energy, pair correlations, and condensate fraction, we expect that, at the two densities considered in Fig. 6, the deviation of the prediction of the big equation from the exact ground state are expected to be smaller than the stochastic error limiting the precision of QMC calculations of the momentum distribution. This is particularly true in the region in which $|\mathbf{k}|^{-4}$ transitions to $|\mathbf{k}|^{-12}$.

E. Nonuniversal behavior at intermediate densities

The low density asymptotics of the energy, given by the Lee-Huang-Yang formula (1), only depend on the potential through the scattering length. At high density (3), they only depend on the potential through $\int d\mathbf{x}\, v(\mathbf{x})$. In this sense, the low and high density behavior of the Bose gas is *universal*. In this section, we show that, at intermediate densities, the energy does not only depend on the scattering length and the integral of the potential, thus suggesting that the behavior of the Bose gas at intermediate densities is *not universal*.

To that end, we have compared the predictions of the big equation for the energy for two potentials that have the same scattering length, and the same integral. The first potential $v_{32}^{(0)}$ is defined in the next section, see (58), and the second is an exponential potential

$$\Phi_{\alpha,\beta}(\mathbf{x}) := \alpha e^{-\beta|\mathbf{x}|} \tag{54}$$

where α and β are chosen in such a way that the scattering length and integral of Φ are equal to those of $v_{32}^{(0)}$. The scattering length of $v_{32}^{(0)}$ was computed numerically and found to be $\approx$0.5878, and its integral is $\frac{64\pi^2}{9}$. The scattering length of $\Phi_{\alpha,\beta}$ is

$$\frac{1}{\beta}\left(\log\frac{\alpha}{\beta^2} + 2\gamma + 2\frac{K_0\left(2\sqrt{\frac{\alpha}{\beta^2}}\right)}{I_0\left(2\sqrt{\frac{\alpha}{\beta^2}}\right)}\right), \tag{55}$$

where γ is the Euler constant and K_0 and I_0 are modified Bessel functions. The integral of $\Phi_{\alpha,\beta}$ is $\frac{8\pi\alpha}{\beta^3}$. We thus find that, in order to make the scattering length and integral of $v_{32}^{(0)}$ and $\Phi_{\alpha,\beta}$ coincide, we must choose $\alpha \approx 907.2$ and $\beta \approx 6.874$.

The prediction of the energy for these two potentials is plotted in Fig. 7. We find that, as expected, the energies coincide at low and high density, but they differ significantly

in the intermediate density regime. We have confirmed this fact by QMC computations, and found good agreement of the QMC data with our prediction for both potentials.

IV. HARD-CORE POTENTIAL

The numerical computations discussed above as well as the proofs in Refs. [20,21] heavily use the assumption that the potential v is integrable, which a priori excludes the case of a hard-core potential, which is infinite inside a radius 1. We have investigated two directions to get around this restriction.

The first, and most straightforward, is to consider the hard-core potential as a limit of soft core potentials. Obviously, this approach will not be accurate at densities approaching close-packing, but as we will see, is rather accurate at smaller densities. As was mentioned in Sec. I, it is preferable to only use potentials of positive type (that is, non-negative potentials with a non-negative Fourier transform). With this in mind, we consider the sequence of potentials

$$v_n^{(0)}(|\mathbf{x}|) := \Theta(1-|\mathbf{x}|)\alpha_n \frac{2\pi}{3}(|\mathbf{x}|-1)^2(|\mathbf{x}|+2), \tag{56}$$

where $\Theta(x)$ is the Heaviside function, which is equal to 1 for $x > 0$ and 0 otherwise, and $\alpha_n \to \infty$. This potential can also be written as

$$v_n^{(0)}(|\mathbf{x}|) = \alpha_n \int d\mathbf{y}\, \Theta\left(\frac{1}{2}-|\mathbf{y}|\right)\Theta\left(\frac{1}{2}-|\mathbf{x}-\mathbf{y}|\right), \tag{57}$$

which shows that it is of positive type because it is the convolution of the function $\Theta(\frac{1}{2}-|\mathbf{x}|)$ with itself. In addition, we fix the scattering length of the potential to 1, by rescaling space: denoting the scattering length of $v_n^{(0)}$ by a_n, we take the potential to be

$$v_n(\mathbf{x}) := v_n^{(0)}\left(\frac{|\mathbf{x}|}{a_n}\right). \tag{58}$$

The second method is to solve the big, medium, and simple equations for $|\mathbf{x}| > 1$, with the boundary condition $u(\mathbf{x}) = 1$ at $|\mathbf{x}| = 1$. From a computational standpoint, the big and Medium equations were too difficult to solve quickly on our hardware. In the case of the simple equation, the computation is much longer than in the case of a soft-core potential, but it is not excessively long. The reason for which solving the equation for $|\mathbf{x}| > 1$ is computationally much more difficult than the soft core case, is that in the latter case, we carry out the computation in Fourier space, in which the big, simple, and Medium equations have fewer integrals. For the hard-core potential, the Fourier transform of u does not decay fast enough for the numerics to be precise, so we work in real space instead, which is computationally more difficult.

In Fig. 8, we compare the predictions for the energy and condensate fraction made using the big, medium, and simple equations to the QMC computation carried out in Ref. [15]. The plots are shown for densities up to the close packing density, which is the maximal allowed density for the hard core potential. All three equations are quite accurate at low density, but the error becomes larger as the density in ramped up. Nevertheless, for the energy, the big equation stays quite close to the QMC simulation. As the density approaches close packing, the potential v_n becomes inadequate. The effects

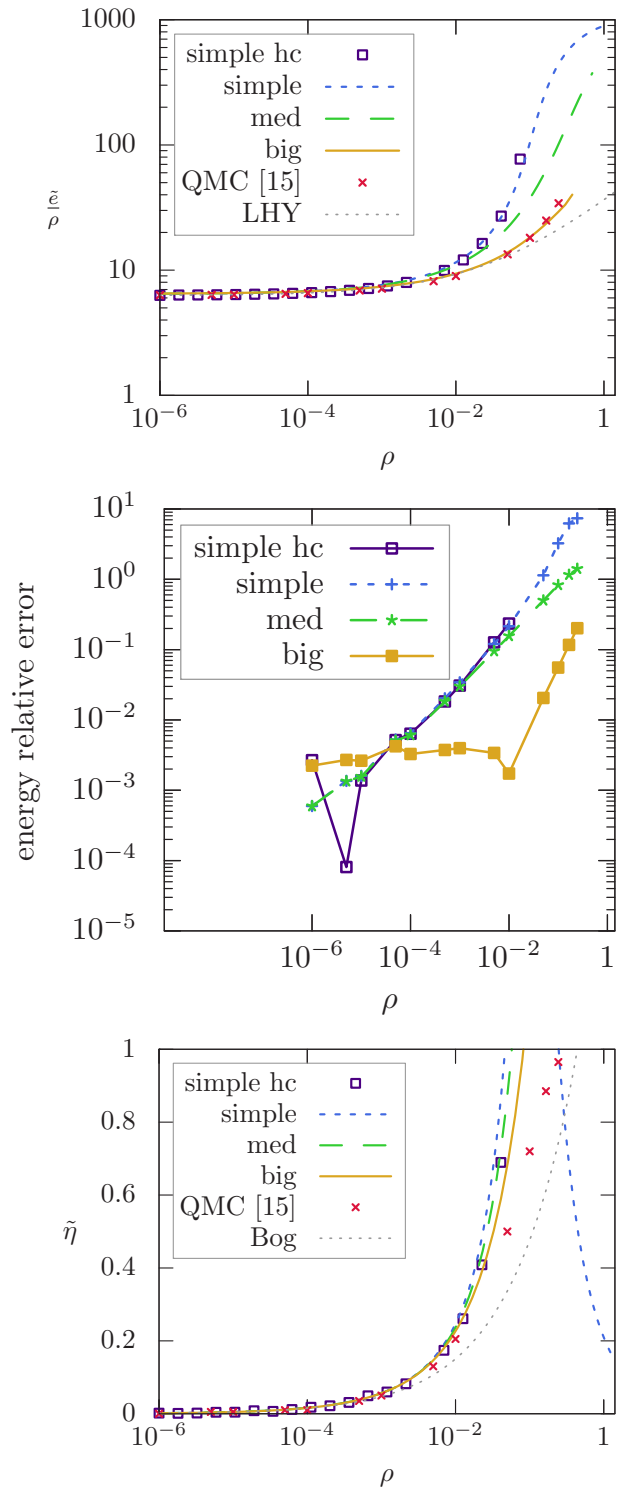

FIG. 8. The energy (top), relative error in the energy $\frac{\tilde{e}-e_{\mathrm{QMC}}}{e_{\mathrm{QMC}}}$ (middle), and noncondensed fraction (bottom) as a function of the density for the hard core potential. The circles were computed by solving the hard core simple equation for $|\mathbf{x}| > 1$ (simple hc). The lines were computed by approximating the hard core potential by the potential $v_{512}(\mathbf{x})$, see (58). We compare the predictions of the big, medium, and simple equations to QMC results reported [15]. The prediction of Bogolubov theory (2) is also plotted for comparison (Bog). The right edge of the plots correspond to the close-packing density $\rho_{\mathrm{cp}} = \sqrt{2}$ [44].

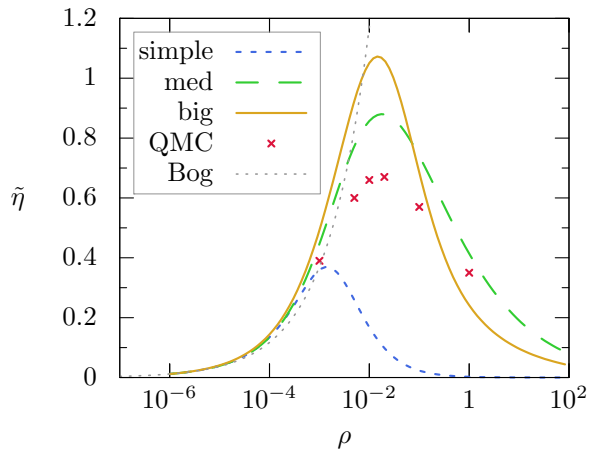

FIG. 9. The noncondensed fraction as a function of the density for the potential $16e^{-|\mathbf{x}|}$. We compare the predictions of the big, medium, and simple equations to a QMC simulation. The prediction of Bogolubov theory (2) is also plotted for comparison (Bog).

of this are most visible for the simple equation. For smaller densities, for the simple equation, we see that the predictions made using v_n are rather close to those made by restricting the equation to $|\mathbf{x}| > 1$.

V. LIMITS OF VALIDITY OF THE SIMPLE EQUATIONS

As we have seen above, the big, medium, and simple equations are, in some cases very accurate (especially the big equation). In this section, we discuss the situations in which these equations make predictions that are far from the QMC simulations, or even unphysical.

First of all, the big, medium, and simple equations are only accurate at high densities if the potential is of positive type, that is, if its Fourier transform is non-negative. Indeed, as we proved for the simple equation in Ref. [20] and as the numerics show for the Big and Medium equations, as $\rho \to \infty$, $\tilde{e} \sim \frac{\rho}{2} \int d\mathbf{x}\, v(\mathbf{x})$. For the Bose gas, this was proved to hold if v is of positive type [2]. It is quite easy to find a counter-example if v is not of positive type. For instance, if $v(\mathbf{x}) = 0$ for all $|\mathbf{x}| < 1$, then, consider a wave function ψ that is smooth and supported on $|\mathbf{x}_1|, \cdots, |\mathbf{x}_N| < \frac{1}{2}$. Since all particles are at a distance that is <1, the potential energy of such a wave function is 0, and its kinetic energy is $O(N)$. Thus, the energy per particle is of order 1, which, for large ρ, is $\ll \frac{\rho}{2} \int d\mathbf{x}\, v(\mathbf{x})$. [Note that a nontrivial, non-negative potential with $v(\mathbf{x})$ cannot be of positive type if $v(0) = 0$, since the maximum of a positive type function is attained at 0].

In addition, we observed that the predictions made by the big, medium, and simple equations get less accurate if the potential is made stronger. Comparing the relative error in Fig. 2 between the potential $e^{-|\mathbf{x}|}$ and $16e^{-|\mathbf{x}|}$ shows that the error is roughly 10 times worse. For the condensate fraction, the situation deteriorates further, as can be seen in Fig. 9, in which we see that, even though the big equation still reproduces the qualitative features of the condensate fraction curve, it yields an unphysical result, with a negative condensate fraction. This is further confirmed by the computations for the hard core potential, in which we see from Fig. 8 that the condensate fraction becomes rather inaccurate at large densities.

VI. CONCLUSIONS

In this paper, we show the good agreement in the predictions of the ground-state energy, condensate fraction and correlation function of the repulsive Bose gas given by the simplified approach developed in 1963 [2] with the values obtained by quantum Monte Carlo calculations, for the potentials $e^{-|\mathbf{x}|}$ and $16e^{-|\mathbf{x}|}$. The simplified approach was thought to be accurate only at low densities, in complete agreement with other analyses of the time. Here, we show that it is accurate at *all* densities. This establishes an alternative approach to many body bosonic physics. Combining this analysis with the exact results in Refs. [20,21] leads us to conjecture that the simplified approach is accurate for any repulsive potential of positive type with a scattering length and an integral that is not too large.

We have discussed three different approximations, the big, medium, and simple equations. The big equation is the most accurate, but also the most difficult to solve. The Medium equation is obtained by neglecting terms of higher order in u, which makes it much more easy to compute with, while remaining rather close to the big equation. The simple equation is then obtained by approximating $g_2(x)v(x)$ by a Dirac-delta function. This drastically simplifies the equation, but is also less accurate at intermediate densities (while the low and high densities are still asymptotically exact).

The simplified approach provides a framework to study the many-body Bose gas directly in the thermodynamic limit, in terms of an equation involving a function of just three variables. The method provides a promising avenue to approach singular potentials, such as the hard core. In addition, this allows us to approach various physical questions, such as Bose-Einstein condensation, even in the intermediate density regime, away from the dilute and dense limits.

ACKNOWLEDGMENTS

We thank two anonymous referees for many helpful comments. E.H.L. thanks the Institute for Advanced study for its hospitality. US National Science Foundation Grants No. DMS-1764254 (E.A.C.) and No. DMS-1802170 (I.J.) are gratefully acknowledged.

[1] W. Lenz, Z. Phys. **56**, 778 (1929).
[2] E. H. Lieb, Phys. Rev. **130**, 2518 (1963).
[3] N. N. Bogolyubov, Izv. Akad. Nauk Ser. Fiz. **11**, 23 (1947).
[4] V. A. Zagrebnov and J.-B. Bru, Phys. Rep. **350**, 291 (2001).
[5] T. D. Lee, K. Huang, and C. N. Yang, Phys. Rev. **106**, 1135 (1957).
[6] E. H. Lieb, in *The Bose Fluid*, Lectures in Theoretical Physics Vol. VIIC (University of Colorado Press, Boulder Colorado, 1965), pp. 175–224.
[7] F. J. Dyson, Phys. Rev. **106**, 20 (1957).
[8] E. H. Lieb and J. Yngvason, Phys. Rev. Lett. **80**, 2504 (1998).

[9] L. Erdős, B. Schlein, and H.-T. Yau, Phys. Rev. A **78**, 053627 (2008).
[10] H.-T. Yau and J. Yin, J. Stat. Phys. **136**, 453 (2009).
[11] A. Giuliani and R. Seiringer, J. Stat. Phys. **135**, 915 (2009).
[12] C. Boccato, C. Brennecke, S. Cenatiempo, and B. Schlein, Acta Math. **222**, 219 (2019).
[13] B. Brietzke and J. P. Solovej, Ann. Henri Poinc. **21**, 571 (2020).
[14] S. Fournais and J. P. Solovej, Ann. Math. **192**, 893 (2020).
[15] S. Giorgini, J. Boronat, and J. Casulleras, Phys. Rev. A **60**, 5129 (1999).
[16] A. Sütő, Commun. Math. Phys. **305**, 657 (2011).
[17] E. Krotscheck, in *Theory of Correlated Basis Functions*, edited by E. K. A. Fabrocini and S. Fantoni, Series on Advances in Quantum Many-Body Theory Vol. 4 (World Scientific, Singapore, 2002), pp. 265–328.
[18] E. H. Lieb and A. Y. Sakakura, Phys. Rev. **133**, A899 (1964).
[19] E. H. Lieb and W. Liniger, Phys. Rev. **134**, A312 (1964).
[20] E. A. Carlen, I. Jauslin, and E. H. Lieb, Pure Appl. Anal. **2**, 659 (2020).
[21] E. A. Carlen, I. Jauslin, and E. H. Lieb [SIAM J. Math. Anal. (to be published)], arXiv:2010.13882.
[22] A. Bijl, Physica **7**, 869 (1940).
[23] R. Dingle, Philos. Mag. **40**, 573 (1949).
[24] R. Jastrow, Phys. Rev. **98**, 1479 (1955).
[25] C. Chin, R. Grimm, P. Julienne, and E. Tiesinga, Rev. Mod. Phys. **82**, 1225 (2010).
[26] V. N. Efimov, Yad. Fiz. **12**, 1080 (1970).
[27] T. Kraemer, M. Mark, P. Waldburger, J. G. Danzl, C. Chin, B. Engeser, A. D. Lange, K. Pilch, A. Jaakkola, H.-C. Nägerl, and R. Grimm, Nature (London) **440**, 315 (2006).
[28] P. Naidon and S. Endo, Rep. Prog. Phys. **80**, 056001 (2017).
[29] Y. Castin and F. Werner, Phys. Rev. A **83**, 063614 (2011).
[30] P. Makotyn, C. E. Klauss, D. L. Goldberger, E. A. Cornell, and D. S. Jin, Nat. Phys. **10**, 116 (2014).
[31] D. H. Smith, E. Braaten, D. Kang, and L. Platter, Phys. Rev. Lett. **112**, 110402 (2014).
[32] C. E. Klauss, X. Xie, C. Lopez-Abadia, J. P. D'Incao, Z. Hadzibabic, D. S. Jin, and E. A. Cornell, Phys. Rev. Lett. **119**, 143401 (2017).
[33] R. J. Fletcher, R. Lopes, J. Man, N. Navon, R. P. Smith, M. W. Zwierlein, and Z. Hadzibabic, Science **355**, 377 (2017).
[34] S. Tan, Ann. Phys. **323**, 2952 (2008).
[35] D. Ruelle, *Statistical Mechanics: Rigorous Results* (World Scientific, Singapore, 1999).
[36] W. L. McMillan, Phys. Rev. **138**, A442 (1965).
[37] M. H. Kalos, Phys. Rev. A **2**, 250 (1970).
[38] D. M. Ceperley, Rev. Mod. Phys. **67**, 279 (1995).
[39] S. Baroni and S. Moroni, Phys. Rev. Lett. **82**, 4745 (1999).
[40] D. M. Ceperley and M. H. Kalos, in *Monte Carlo Methods in Statistical Physics* (Springer, Berlin, Heidelberg, 1986), pp. 145–194.
[41] M. Ruggeri, S. Moroni, and M. Holzmann, Phys. Rev. Lett. **120**, 205302 (2018).
[42] M. Holzmann, R. C. Clay, III, M. A. Morales, N. M. Tubman, D. M. Ceperley, and C. Pierleoni, Phys. Rev. B **94**, 035126 (2016).
[43] R. Combescot, F. Alzetto, and X. Leyronas, Phys. Rev. A **79**, 053640 (2009).
[44] T. Hales, Ann. Math. **162**, 1065 (2005).